PHYSICAL REVIEW B VOLUME 12, NUMBER 7 1 OCTOBER 1975

Spin-wave analysis of specific heat and magnetization in EuO and EuS

O. W. Dietrich
Research Establishment Risø, DK-4000 Roskilde, Denmark

A. J. Henderson, Jr.* and H. Meyer
Department of Physics, Duke University, Durham, North Carolina 27706

(Received 23 April 1975)

Recent neutron scattering measurements of the spin-wave spectrum have shown that the second-nearest-neighbor exchange constant in EuO is ferromagnetic, in disagreement with previously published results from both specific-heat and magnetization measurements. We undertook a thorough study of the bulk data on both EuO and its isomorph EuS, including some previously unpublished specific-heat data. The new analysis resolved the controversy regarding the specific heat, which is actually in good agreement with the neutron scattering results. However, the NMR data are more sensitive to effects other than the exchange energy, making this technique inferior to the two other techniques regarding determination of the exchange constants. We obtained a set of "recommended" values for the nearest- and next-nearest-neighbor exchange constants in EuO and EuS. For EuO they are $J_1/k = 0.606 \pm 0.008$ and $J_2/k = 0.119 \pm 0.015$; and for EuS they are $J_1/k = 0.228 \pm 0.004$ and $J_2/k = -0.102 \pm 0.005$.

I. INTRODUCTION

In the study of magnetism, the europium chalcogenides constitute an interesting group of materials. This is partly because they exhibit a high degree of symmetry and isotropy as well as short-range magnetic interaction, making them simple model systems, and partly because the only structural difference between them is the size of the anion, which enables a study of the radial dependence of the exchange forces. This dependence is most obvious in the change from ferromagnetic to antiferromagnetic order which appears when going from the light anion in EuO towards the heavy anion in EuTe. Kasuya[1] attempted a theoretical analysis of the first- and second-neighbor exchange mechanisms. His conjectures were based on experimental evidence from measurements of transition temperatures, specific heat,[2,3] and magnetization.[4,5] The postulated exchange mechanisms generally describe the observations quite satisfactorily except for the second-neighbor exchange constant J_2 in EuO, which Kasuya suggested should be positive (ferromagnetic), in contradiction to the published analyses of the bulk measurements which determined J_2 to be negative (antiferromagnetic). Recently, neutron scattering measurements of spin-wave spectra in EuO and[6] EuS gave a more direct determination of the two significant exchange constants in these materials. The new observations did confirm the theoretical conjecture of a positive J_2, but, of course, raised the question of why the bulk measurements gave a different answer.

We renalyzed the specific-heat and magnetization measurements and found that the bulk data in EuO only determine the spin-wave stiffness constant, i.e., the sum of the nearest-neighbor (nn) and next-nearest-neighbor (nnn) exchange constants. The new analysis shows that this quantity is in agreement with the neutron scattering result, thus resolving the controversy. Details of our analysis applied to both EuO and EuS are presented in Secs. II and V. Some of the data that we analyzed on specific heat have not previously been reported. Therefore, in Secs. III and IV, we describe the experimental details and present all the data for these measurements.

II. SPIN WAVES IN EUROPIUM CHALCOGENIDES

A. Exchange interaction

The europium chalcogenides crystallize with the rock salt structure in which the magnetic ions form fcc lattices. The spin $S = \frac{7}{2}$ of the Eu^{2+} ion is due to the $4f$ electrons, whose wave functions are strongly localized with no direct overlap between neighboring ions. According to Kasuya,[1] the exchange between nn Eu^{2+} ions is due to an indirect exchange via the normally unoccupied $5d$ conduction bands. The next-nearest neighbor is shielded by an anion, and the exchange coupling between nnn Eu^{2+}ions is thought to involve several mechanisms. One is a superexchange in which the anion p electron is involved, and another is the formation of Eu^{3+}-Eu^{+} nnn pairs by transfer of a $4f$ electron. We refer to the paper of Kasuya for a detailed discussion of these mechanisms and of their dependence on the interionic distance, which dependence causes the interesting change of magnetic behavior within the series of the europium chalcogenides.

For the present we only need to note that the Eu^{2+} ions in the spherically symmetric $^8S_{7/2}$ spin states arranged in the lattices of high symmetry give rise to an isotropic exchange interaction with nn and nnn, which can be written in the Heisenberg form

$$H_{\text{exch}} = -\sum_{\text{nn}} J_1 \vec{S}_0 \cdot \vec{S}_{\text{nn}} - \sum_{\text{nnn}} J_2 \vec{S}_0 \cdot \vec{S}_{\text{nnn}} , \tag{1}$$

where J_1 and J_2 are the two exchanges constants and $\vec{S}_0$, $\vec{S}_{\text{nn}}$, and $\vec{S}_{\text{nnn}}$ are the spins at the origin, at nn and at nnn positions, respectively. With this Hamiltonian the spin-wave energy takes a simple form in the fcc lattice:

$$E_{\text{exch}} = 2S\Big(12J_1 + 6J_2 - J_1 \sum_{\text{nn}} \cos(\vec{q}\cdot\vec{r}_{\text{nn}}) - J_2 \sum_{\text{nnn}} \cos(\vec{q}\cdot\vec{r}_{\text{nnn}})\Big) . \tag{2}$$

For small q, the exchange energy becomes isotropic and characterized by a single parameter, the stiffness constant $D = 4Sr_{\text{nn}}^2(J_1 + J_2)$. Expansion of Eq. (2) for small q yields $E_{\text{exch}} \simeq Dq^2$.

B. Other contributions to spin-wave energy

For general $\vec{q}$ values, the spin-wave energies are dominated by E_{exch}, but at small $\vec{q}$ values the dipolar contribution affects the spectrum significantly. The combined exchange-dipolar spin-wave energy was evaluated by Keffer,[7]

$$\hbar\omega_q = (A_q^2 - |B_q|^2)^{1/2} , \tag{3}$$

where

$$A_q = g\mu_B H_{\text{ext}} + E_{\text{exch}} + N(g\mu_B)^2 S[D^{zz}(0) + \tfrac{1}{2}D^{zz}(\vec{q})] , \tag{4}$$

$$B_q = -\tfrac{1}{2}N(g\mu_B)^2 S[D^{xx}(\vec{q}) - D^{yy}(\vec{q}) - 2iD^{xy}(\vec{q})] , \tag{5}$$

with

$$D^{ij}(\vec{q}) = \frac{1}{N}\sum_{l}{}' (3r_l^i r_l^j - r_l^2 \delta_{ij}) r_l^{-5} \exp(i\vec{q}\cdot\vec{r}_l) . \tag{6}$$

Here the z axis is along the preferred spin direction, and H_{ext} represents the external field. Neither the exchange nor the dipolar forces has a preferred spin direction, but there is a small anisotropic crystalline field which stabilizes the spins in the ground state along $\langle 111 \rangle$ directions.[8,9] This in turn creates a small energy gap that was evaluated[6] from the anisotropy constants to be 0.0035 meV in EuO and an order of magnitude smaller in EuS. For the measurements discussed in this paper a gap of this magnitude is insignificant, but the existence of the preferred spin direction is of importance for the dipolar terms.

The dipolar terms in Eqs. (4) and (5) are sums over the spin sites within the magnetic domains. For finite values of $\vec{q}$, $D^{ij}(\vec{q})$ is essentially independent of the domain shape, but this is not true for $D^{zz}(0)$, which appears in Eq. (4). The convergence of this term is so slow that it depends on the summation boundary. It is customary to treat $D^{zz}(0)$ as follows. The sum is divided into two parts, one containing the sites within a sphere of arbitrary radius, but confined within the domain, the other containing the sites outside the sphere. The summation of the sphere can be performed exactly, and for cubic crystals like EuO and EuS the sum actually vanishes. The summation outside the sphere is first transformed into a volume integral and further into two surface integrals, one over the "inner" sphere surface and the other over the "outer" domain surface. The integral over the sphere is the well-known "Lorentz factor" of $\frac{4}{3}\pi$, and the integral over the domain surface is the demagnetization factor $-\mathfrak{D}$. For cubic crystals $D^{zz}(0)$ thus has the form

$$D^{zz}(0) = \tfrac{4}{3}\pi - \mathfrak{D} . \tag{7}$$

In zero external field the energetically most favorable domain shape is a long thin needle, which minimizes the external field energy. For an unmagnetized sample the needles are packed antisymmetrically, so as to give vanishing total magnetization. We shall assume that our sample in zero field exhibit this type of domain for which $\mathfrak{D} = 0$. In nonzero external fields the domain configuration changes and $\mathfrak{D}$ is nonvanishing. In this case the external field and the demagnetization field combine to an internal field

$$H_{\text{int}} = H_{\text{ext}} - Ng\mu_B S\mathfrak{D} = H_{\text{ext}} - M\mathfrak{D} . \tag{8}$$

The demagnetization field will cancel the external field up to a certain value of the external field, and only then will the internal field become different from zero. In Fig. 4, we show evidence of this behavior of the internal field.

The q-dependent terms $D^{ij}(\vec{q})$ can be summed in a straightforward fashion for q close to the zone boundary $q_{\max}$. For $q \lesssim 0.1q_{\max}$, however, the convergence is slow and it is necessary to employ either the Ewald summation technique or the Holstein-Primakoff (HP) approximation.[7,10] The Ewald technique improves the convergence by transforming part of the sum into a sum over the reciprocal lattice. We have used this technique in the form described by Cohen and Keffer.[11] In the HP approximation $D^{ij}(\vec{q})$ is expanded as follows:

$$D^{ij}(\vec{q}) = (\tfrac{4}{3}\pi)[\delta_{ij} - 3q_iq_j/q^2 + \mathcal{O}(q^2) + \cdots] . \quad (9)$$

Neglecting terms of order q^2 and higher, the spin-wave energy takes the simple form

$$\hbar\omega_q = (g\mu_B H_{\text{int}} + E_{\text{exch}})\left(1 + \frac{4\pi g\mu_B M}{g\mu_B H_{\text{int}} + E_{\text{exch}}} \sin^2\theta_q\right)^{1/2} , \quad (10)$$

where θ_q is the angle between $\vec{q}$ and the preferred spin direction. In Table I, we have compared the exact Ewald summation with the HP approximation [Eq. (10)] for various points in the Brillouin zone. The scale of q is such that the zone boundary in the [100] direction corresponds to $q_x = 0.5$. It is evident from Table I that the HP approximation is extremely good over the entire Brillouin zone, the deviation from the exact summation being always less than 0.5%. Equation (10) is therefore used when calculating the Brillouin-zone sums for the specific heat and magnetization, as discussed in Sec. II C.

C. Magnetization and specific heat

At finite temperatures spin waves are thermally excited, whereby the magnetization is reduced below saturation. The creation of one spin wave causes a spin to flip by one unit. Thus the relative magnetization is

$$\frac{\Delta M}{M} = \frac{1}{NS}\sum_q \langle n_q\rangle , \quad (11)$$

where N is the number of spins and $\langle n_q\rangle$ is the number of excited spin waves given by the Bose distribution function $[\exp(\hbar\omega_q/kT) - 1]^{-1}$. The sum in Eq. (11) is taken over the N $\vec{q}$ values of the Brillouin zone. The magnetic specific heat per spin C_M is the temperature derivative of the magnetic energy per spin, i.e.,

$$C_M = \frac{1}{N}\sum_q \frac{\partial}{\partial T}(\langle n_q\rangle \hbar\omega_q)$$
$$= \frac{kT}{N}\sum_q\left(\frac{\hbar\omega_q}{kT}\right)^2 \exp\left(\frac{\hbar\omega_q}{kT}\right)\left[\exp\left(\frac{\hbar\omega_q}{kT}\right) - 1\right]^{-2} . \quad (12)$$

With the spin-wave energy given by Eq. (10) the summations in Eqs. (11) and (12) can be performed numerically on a computer. The computation time is reduced by utilizing the symmetry within the Brillouin zone. The exchange energy itself is fully described in $\frac{1}{48}$ of the zone (e.g., the volume between the directions [100], [110], and [111]). But for each $\vec{q}$ vector in this volume there are four equally possibly and energetically nonequivalent orientations of the easy spin direction, namely, [111], $[11\bar{1}]$, $[1\bar{1}1]$, and $[\bar{1}11]$, each of which generally give a different value of $\sin^2\theta_q$ in Eq. (10). We have subdivided the volume of summation in cubical boxes, accounting for the reduction of volume (or weight) of boxes on edges and surfaces. It was checked numerically that the summation net (box size) was sufficiently small so that the calculated quantities, i.e., the magnetization or the specific heat, were independent of any further reduction of net size. With the q scale specified in Table I a box side length of 0.02 was generally satisfactory.

We found it informative to determine which portions of the Brillouin zone actually contribute to the magnetic specific heat and to the reduced magnetization. Therefore, in Fig. 1,

$$\frac{\partial(C_M/R)}{\partial q} \text{ and } \frac{\partial(\Delta M/M)}{\partial q}$$

TABLE I. EuO: Effect of the dipolar contribution to the spin-wave energy calculated by the Ewald summation technique and by the HP approximation.

Wave vector			Spin-wave energy (meV)		
q_x	q_y	q_z	Pure exchange	Ewald summation	HP approximation
0.01	0	0	0.0069	0.0365	0.0364
0.05	0	0	0.1706	0.2469	0.2463
0.10	0	0	0.6580	0.7454	0.7448
0.50	0	0	5.8510	5.9436	5.9428
0.01	0.01	0	0.0138	0.0384	0.0383
0.05	0.05	0	0.3377	0.3817	0.3812
0.10	0.10	0	1.2626	1.3099	1.3080
0.375	0.375	0	6.0128	6.0939	6.0589
0.01	0.01	0.01	0.0207	0.0207	0.0207
0.05	0.05	0.05	0.5013	0.5026	0.5013
0.10	0.10	0.10	1.8138	1.8182	1.8138
0.25	0.25	0.25	5.2500	5.2627	5.2500

are plotted for EuO at 2 and 4 K. It is immediately seen that the significant contribution to the specific heat in this temperature range, which is typical of our measurements, comes from the region in the Brillouin zone where the exchange energy is characterized solely by the stiffness constant D. Therefore, these measurements cannot be expected to determine J_1 *and* J_2, but only $J_1 + J_2$. We note, however, that there is a considerable shift of

$$\frac{\partial(C_M/R)}{\partial q}$$

towards larger q values in going from 2 to 4 K. Had the measurements been extended up to about $0.25T_c$ (i.e., about 17 K), the specific heat would sense the whole of the Brillouin zone. Hence in EuS, where the measurements were again taken below 4.3 K, the analysis of the specific heat should yield both J_1 and J_2 because T_c is only 16.6 K in this material.

Now considering the reduced magnetization, the situation is even worse. At both 2 and 4 K the region of the Brillouin zone that contributes to the sum in Eq. (11) is confined around the origin and there is only a minor change from 2 to 4 K. We conclude therefore that the NMR data below 4 K in EuO are sensitive only to the spin-wave energy at very-small q values, where the dipolar energy and the energy gap play an important role.

The considerations relating to Fig. 1 about the limitations of the information in the bulk measurements were not realized in the previously published analyses of these data,[2,4] in which *both* J_1 and J_2 were stated with high accuracy. The misinterpretation would have become evident through a proper treatment of the correlated uncertainties of J_1 and J_2.

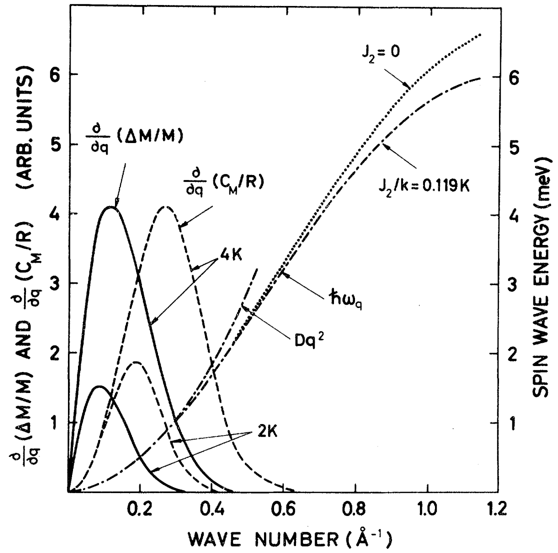

FIG. 1. Sensitivity of specific-heat and NMR measurements to J_1 and J_2. The dashed-dotted line represents spin-wave dispersion in the [110] direction for EuO using the values determined by neutron scattering for J_1 and J_2. The dotted curve has the same stiffness constant $D \propto (J_1 + J_2)$, but $J_2 = 0$. It is evident that the individual values of J_1 and J_2 are important only within the second half of the Brillouin zone (BZ). Solid curves represent the calculated contribution from different q shells in the BZ to the reduced magnetization at 2 and 4 K as measured by NMR. Likewise, dashed curves are the differential contribution to the specific heat. Both techniques applied below 4 K only sample the inner half of the BZ, and therefore they only determine $J_1 + J_2$. In addition, the NMR measurements are particularly dependent on the dipolar energy dominating at the lowest q values.

At temperatures where $\Delta M/M$ differs significantly from zero it is necessary to account for the renormalization of the spin wave energies. For temperatures not too close to the critical temperature T_c, and for large spins, the renormalization is dominated by the dynamical spin-wave interaction. In calculating the relative renormalization we have followed the treatment given by Marshall and Lovesey[12] for a purely exchange-coupled magnet. Thus the dipolar energy is neglected in this calculation, but we have reasons to believe that this causes only a minor error because the same calculation agrees with the spin-wave renormalization measured by the neutron scattering[13] for temperatures up to 0.8 T_c in EuO. The renormalization of the exchange energy can be expressed in terms of separate renormalizations of the individual exchange constants. Hence Eq. (2) remains valid at all temperatures; only the values of J_1 and J_2 vary with temperature. The relative changes of J_1 and J_2 are given by

$$\frac{J_1(T)}{J_1(T=0)} = 1 - \frac{1}{SN} \sum_q \left(1 - \tfrac{1}{6} \sum_{\text{nn}} \cos(\vec{q}\cdot\vec{r}_{\text{nn}})\right)\langle n_q\rangle \;,$$

$$\frac{J_2(T)}{J_2(T=0)} = 1 - \frac{1}{SN} \sum_q \left(1 - \tfrac{1}{3} \sum_{\text{nnn}} \cos(\vec{q}\cdot\vec{r}_{\text{nnn}})\right)\langle n_q\rangle \;. \tag{13}$$

Since on the right-hand side $\langle n_q\rangle$ is the Bose function for the renormalized energies, the computation must be carried out self-consistently. Typically, at low temperatures the relative renormalization is about one-half of the relative change in the magnetization. In EuO, where $T_c = 69.2$ K, the renormalization is insignificant for temperatures below 4.2 K. In EuS, with $T_c = 16.6$ K, the relative renormalization amounts to about 2% at 4.2 K.

III. EXPERIMENTAL

A. Cryostat

The cryostat used in the experiments was that described previously,[14] and therefore no detailed description will be given here. The available temperature region was between 0.35 and 4.3 K. The sample was fastened by threads to a support, a small amount of vacuum grease being used to improve the thermal contact. This support could be brought into contact with the refrigerant bath by means of a mechanical heat switch. Any horizontal displacements were prevented by fastenings along the side of the cryostat. Two carbon thermometers, attached to the sample support, were used to monitor the temperature and were calibrated against the vapor pressure of ^{3}He and ^{4}He and as a function of the applied field.

B. Samples

The samples were all prepared by Reed at Lincoln Laboratories. A summary of the samples used in the experiments is seen in Table II.

EuO. The EuO material was prepared from a melt of Eu_2O_3 and Eu metal, as described by Shapira and Reed.[15] The two crystals listed were grown in different batches. In another crystal grown by the same techniques, the major impurities found by mass-spectrometric analysis were (in ppm atomic percent) C: 90; Ca: 60; Yb: 40, and N: 13. EuO is chemically active and forms a film of oxyhydroxide and trihydroxide on its surface when exposed to moist air.[16] Hence precautions were taken to keep the samples packed in dessicant until they were sealed in the cryostat. The good consistency between the calorimetric results of both samples 1 and 2 suggests that there was little if any deterioration between the time of preparation and the experiment.

Sample 2 was suspended in the cryostat so that the applied magnetic field was parallel to the approximately flat surface of the slab, thus giving a minimum demagnetization factor. The irregular shape of the crystal, however, prevented an accurate calculation of the demagnetization field, which was determined empirically from the experiment (see the end of Sec. IV).

To study possible surface effects in the specific heat due to magnetic surface modes,[17] another sample was prepared by grinding crystalline chips to a fine powder in an argon atmosphere. The powder was then mixed with a clear epoxy to prevent a chemical reaction. In spite of the precautions taken, there must have been some contamination as evidenced by a large peak in the specific heat at 2.1 K. Hence, further studies on this sample were discontinued.

EuS. The first calorimetric attempt was made with a sample consisting of two single crystals. However, these experiments had to be abandoned because of very-large thermal relaxation times encountered during the measurements: After a heating pulse it took the sample more than 10 min to reach an equilibrium temperature near 3 K, this time increasing considerably as the temperature was decreased. A powdered sample with an average individual particle size smaller than 38μ and cast into Ward bioplastic was prepared. Presumably because EuS has a higher chemical stability than EuO, this sample showed no specific heat anomaly and its thermal relaxation times remained less than a few minutes over the whole range of temperatures.

C. Errors

A reasonable estimate of all sources of error indicates that there is an absolute uncertainty of about ± 2%. The major sources of systematic

TABLE II. Summary of sample details. The quantity $p(T)$ is the ratio of the addenda heat capacity to that of the sample, and is expressed as a fraction at $T(K)$.

Sample	Composition	Shape	Mass (g)	$p(1)$	$p(4)$
1	EuO single crystal	Flat cylinder diameter 0.51 cm height 1.13 cm	4.19	0.14	0.17
2	EuO single crystal	Slab of 0.3 mm thickness and ~1.5 cm diameter	3.15	0.18	0.22
3	EuS	Powder cast in epoxy	1.27	0.01	0.08

error in the specific heats in the experiments arise (i) from the slope S of the thermometer calibration curve, estimated to be about $\delta S/S \simeq 1\%$, and (ii) from the heat capacity of the addenda, namely, sample support, grease, sample plastic casing, threads, etc., measured in a separate experiment to about 2% accuracy. For all the samples this additional heat capacity was at most 30% of that of the sample.

As mentioned in a previous publication,[14] the present calorimeter and the experimental techniques were tested by measuring the specific heat of high-purity copper. The agreement between these measurements and the most reliable ones made on[18] Cu (a difference of about 1.5% and less than 0.5% at 1 K and above 3 K, respectively) should be considered good enough for the purposes of the present research.

IV. CALORIMETRY RESULTS FOR EuO AND EuS

Several hundred points were obtained altogether for the specific heat of the two EuO samples 1 and 2 at zero magnetic field,[19] for sample 2 at 12.9 kOe, and for the EuS-powder sample at zero magnetic field. This amount of data is too voluminous to be presented here, and instead we have tabulated smoothed results at suitable temperature intervals. In general, the scattering of the data around the smoothed values is of the order of ± 1% in zero field, and a few percent in the applied field in the lowest temperature region. The smoothed results are listed in Table III, whereas all experimental points for EuO and EuS are shown in Figs. 2 and 3, respectively. There is good consistency between both EuO samples, and agreement between the present data and those of Passenheim, McCollum, and Callaway.[3]

One expects three additive contributions to the specific heat of EuO and EuS, namely,

$$C = C_M + C_L + C_N , \tag{14}$$

where C_M, C_L, and C_N refer, respectively, to the magnetic excitations, the lattice vibrations, and the hyperfine splitting of the ^{151}Eu and ^{153}Eu nuclei. The respective proportions of these isotopes are 47.86% and 52.14%, their nuclear magnetic moments are $3.4\mu_N$ and $1.5\mu_N$, and their nuclear spin is $\frac{5}{2}$.[20]

The lattice contribution C_L for both EuS and EuO has been assumed to follow a Debye T^3 law with $\Theta_D = 350$ K determined from ultrasonic measurements in EuO.[15] We obtain

$$C_L/R = 1.1\times 10^{-3} T^3 \ . \tag{15}$$

This contribution is only a small fraction of C/R in EuO, and is still smaller in EuS.

TABLE III. Smoothed specific heats of EuO and EuS expressed as $(C/R)\times 10^3$.

	EuO single crystals			EuS
	$H=0$		$H=12.9$ kOe	powder
T(K)	No. 1	No. 2	No. 2	$H=0$
0.40	2.65			
0.45	2.35			
0.50	2.14			
0.55	1.99			
0.60	1.91	1.89	1.27	15.3
0.70	1.86	1.83	1.18	18.7
0.80	1.93	1.89	1.24	22.8
0.90	2.07	2.07	1.40	27.0
1.0	2.31	2.30	1.60	31.9
1.1	2.59	2.56	1.87	37.2
1.2	2.91	2.89	2.15	42.7
1.4	3.65	3.62	2.75	56.6
1.6	4.48	4.43	3.48	71.7
1.8	5.45	5.32	4.23	88.3
2.0	6.50	6.28	5.10	107.5
2.2	7.58	7.38	6.05	129.6
2.4	8.80	8.58	7.04	154.6
2.6	10.15	9.90	8.20	180.6
2.8	11.6	11.3	9.45	209.3
3.0	13.2	12.9	10.9	238.1
3.2	14.8	14.5	12.4	268.8
3.4	16.6	16.2	14.0	299.5
3.6	18.4	18.0	15.7	328.3
3.8	20.2	19.9	17.5	355.2
4.0	22.0	21.8	19.5	380.2
4.2	23.9	23.7	21.3	404.2
4.4	25.7	25.6		

The nuclear contribution is calculated from

$$\frac{C_N T^2}{R} = \sum_i n_i \tfrac{1}{3}[I_i(I_i+1)]\left(\frac{\Delta_i}{k_B}\right)^2 , \tag{16}$$

where n_i, I_i, and Δ_i are the fraction, the spin, and the nuclear splitting of the isotope i. From NMR data[4,5] in ^{153}Eu, and the ratio of the nuclear magnetic moments, we calculate

$$C_N T^2/R = 3.85\times 10^{-4} \text{ for EuO}, \tag{17a}$$

$$C_N T^2/R = 4.61\times 10^{-4} \text{ for EuS}. \tag{17b}$$

In EuO, the nuclear contribution dominates at temperatures below about 0.7 K, as can be seen in Fig. 2. Assuming that C_M will be approximately proportional to $T^{3/2}$, which is the dependence of a simple ferromagnet at sufficiently low temperatures, a data plot of CT^2/R vs $T^{7/2}$ will be expected to give a nearly straight line. The intercept at $T=0$, namely, $C_N T^2/R$, should be consistent with the value in Eq. (17a), which is shown to be correct in the insert of Fig. 2. For EuS, the nuclear contribution is just a small correction

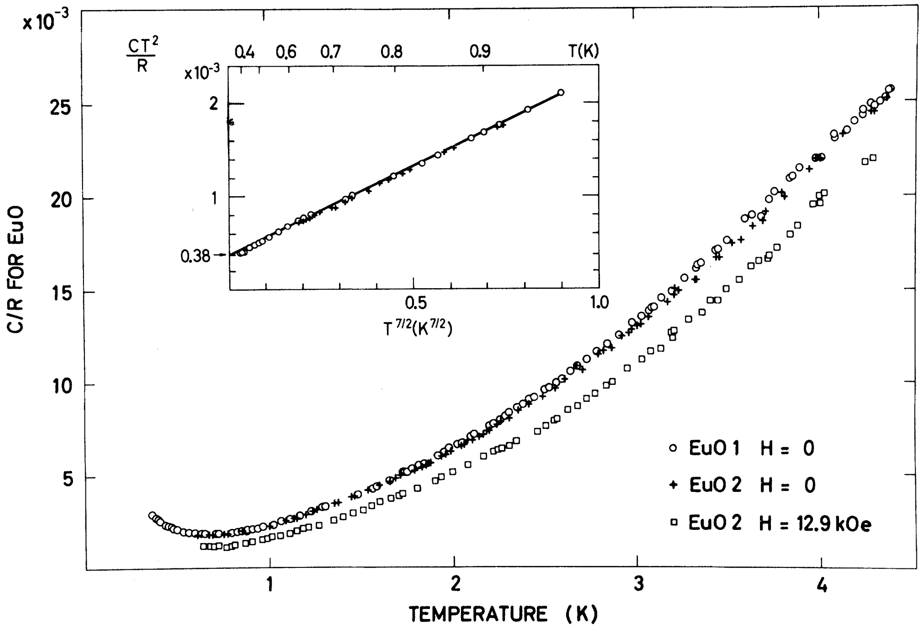

FIG. 2. Total specific heat vs temperature for two EuO samples at zero field and for one of the samples at an external field of 12.9 kOe. The insert shows the low-temperature zero-field data multiplied by T^2 and plotted vs $T^{7/2}$. The intercept at $T=0$ determines the nuclear specific heat, as explained in text.

of C accounting for only 8% at 0.6 K.

Two additional series of calorimetric data for EuO, sample 2, were obtained near 0.70 and 3.45 K, respectively, for various external fields between 5.1 and 12.5 kOe. The data for the isotherms at these temperatures are presented in reduced form in Fig. 4. It can be seen that for $H_{\text{ext}}=4.8$ kOe, the data extrapolate to the value at zero field. Hence we take 4.8 kOe to be the maximum demagnetization field and write

$$H_{\text{int}}=H_{\text{ext}}-4.8\text{ kOe}\quad\text{for } H_{\text{ext}}>4.8\text{ kOe},\qquad H_{\text{int}}=0\quad\text{for } H_{\text{ext}}<4.8\text{ kOe}. \tag{8a}$$

These results are discussed in Sec. V.

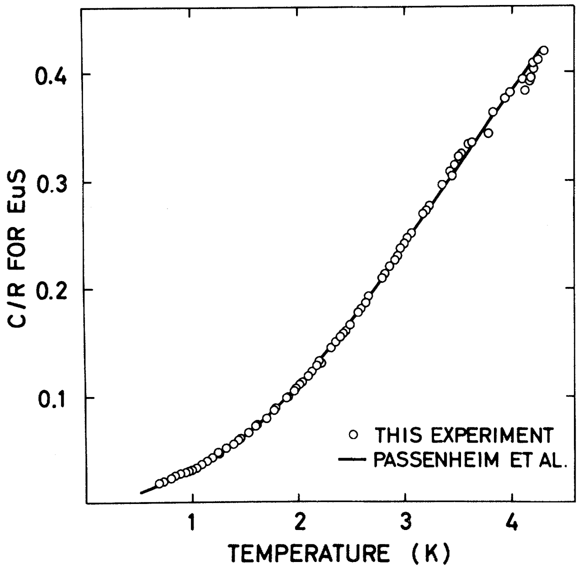

FIG. 3. Total specific heat of EuS vs temperature. The figure shows the good agreement between our data, represented by open circles, and the data of Passenheim, McCollum, and Callaway (Ref. 3), represented by the solid curve.

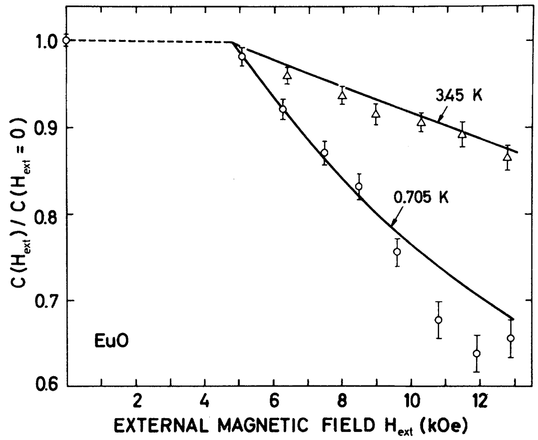

FIG. 4. Isotherms in EuO at 0.705 and 3.45 K. Points represent our measurements of the relative decrease of the total specific heat with increasing field. No change of specific heat is observed until the field exceeds 4.8 kOe. Therefore, we have taken this value to be the demagnetization field. Solid curves are the calculated isotherms.

V. RESULTS

Section II described the calculation of the spin-wave energy $\hbar\omega_q$, the magnetic specific heat C_M, and the reduced magnetization $\Delta M/M$. We shall now discuss the analysis of the measured temperature variations of C_M and $\Delta M/M$.

A. Specific heat

Having subtracted the nuclear and lattice contributions from the measured total specific heat, the resulting magnetic specific heat was least-squares fitted to Eq. (12), using the exchange constants as free variables. That is, at each temperature the specific heat was calculated for a certain set of exchange constants (J_1, J_2), and then J_1 and J_2 were varied so as to give a minimum of the summed squared deviations.

As already anticipated in connection with Fig. 1, the fitting procedure fails to determine two unique exchange constants in the case of EuO, evidently because the measurements do not sample the entire Brillouin zone. We have therefore instead fitted the EuO data with a single parameter, namely, $J_1 + J_2$, which is proportional to the stiffness constant governing the low-q behavior of the spin-wave energy. The best fit is shown as the curve marked $H_{\text{ext}} = 0$ in Fig. 5. To better display the discrepancies between calculated and measured specific heats, which would not be easily seen in a linear scale, $C_M/RT^{3/2}$ is plotted versus T. For a purely exchange-coupled ferromagnet, this quantity would show a linear variation with T, because for small T, C_M/R expands as[21]

$$C_M/R = AT^{3/2} + BT^{5/2} + \cdots . \tag{18}$$

Equation (18) is plotted as a dashed line in Fig. 5. The difference between this line and the solid curve marked $H_{\text{ext}} = 0$ illustrates the importance of the dipolar effect. At 0.6 K, the inclusion of the dipolar energy almost halves the magnitude of the specific heat with respect to that of the purely exchange-coupled magnet.

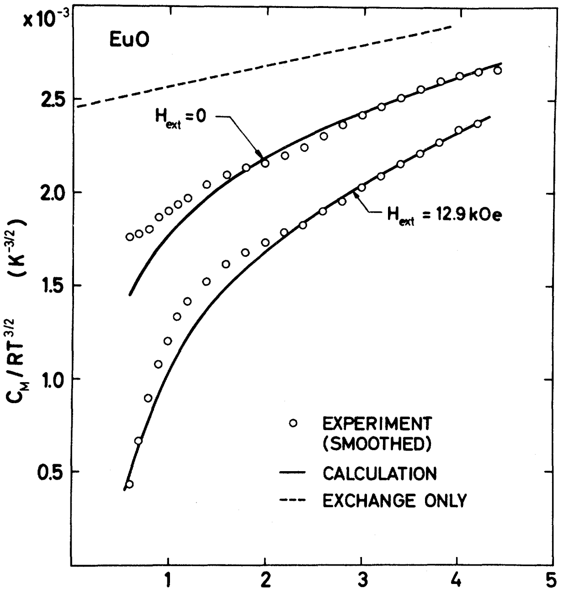

FIG. 5. Magnetic specific heat divided by $T^{3/2}$ vs temperature in EuO. In this type of plot the specific heat of a purely exchange-coupled ferromagnet will vary linearly, as indicated by the dashed line. The reduction of $C_M/RT^{3/2}$ below this line is a result of the dipolar effect on the spin-wave energy. Solid curve marked $H_{\text{ext}} = 0$ is the best fit to the zero-field data for $(J_1 + J_2)/k = 0.714$. The lower curve is calculated with this value of $J_1 + J_2$ and an external field of 12.9 kOe.

Viewed in this perspective, we find the over-all agreement between the calculated and the measured specific heat good, noticing that the calculation contains only one adjustable parameter. However, below 1.5 K, a systematic deviation develops which we cannot account for. We tend to discard the possibility of an incorrect estimation of the addenda in the heat-capacity measurements or of a systematic error in the temperature scale, because other compounds measured in the same cryostat gave results in agreement with published values. There is a possibility of impurities in the samples, caused from surface contamination, and lastly there is still the possibility that theory does not account entirely for the bulk properties of our samples below about 1 K, although admittedly there is an excellent agreement with the data for EuS by Passenheim *et al.* over the whole temperature range, as we shall discuss later. Since the discrepancy we are referring to is relatively small, and of little influence for the determination of $J_1 + J_2$, we have not given it further attention. The best value of the sum of the two exchange constants is

$$(J_1 + J_2)/k = 0.714 \pm 0.007\ \text{K}. \tag{19}$$

The uncertainty is the statistical uncertainty from the fitting procedure and does not include possible systematic errors, for which we have no good estimates. The quoted value compares favorably with that determined by neutron scattering,[6] which yielded $J_1/k = 0.606 \pm 0.008$ K and $J_2/k = 0.119 \pm 0.015$ K. Adding J_1 and J_2 and taking account of the correlation between the uncertainties, we find

$$(J_1 + J_2)/k = 0.725 \pm 0.006\ \text{K}. \tag{20}$$

For the best value of $J_1 + J_2$ we have calculated the magnetic specific heat in an external field of 12.9 kOe, using a demagnetization field of 4.8 kOe to find the internal field, Eq. (8a). The result is shown as the lower curve in Fig. 5. The agreement with the measurements is extremely good above 2 K considering that the calculation contains no adjustable parameters in this case. But here again we sample additional specific heat below 2 K.

The isotherms at 0.705 and 3.45 K were also calculated as shown in Fig. 4. The agreement with the measured isotherms is good except for a few points at 0.705 K, which could be experimental error. Thus in spite of the 13% discrepancy between the calculated and the measured specific heat at 0.705 K and zero field, it appears that the relative change with field is correctly accounted for in our calculations.

The results of the analysis of the magnetic specific heat in EuS are shown in Fig. 6, where we have plotted $C_M/RT^{3/2}$ vs T (notice the suppressed zero on the ordinate scale). The points are smoothed experimental data both from this experiment and from the experiment by Passenheim, McCollum, and Callaway,[3] corrected by us for the nuclear and lattice contributions. The full curve is the best fit to the filled circles (Passenheim *et al.*), and the agreement is excellent over the whole temperature range. In the insert in Fig. 6 is shown the covariance ellipse for the fit parameters, giving the correlated uncertainties for the exchange constants J_1 and J_2. The resulting values of J_1 and J_2 are

$$J_1/k = 0.228 \pm 0.003 \text{ K}, \quad J_2/k = -0.102 \pm 0.005 \text{ K}. \tag{21}$$

These numbers deviate somewhat from those quoted by Passenheim *et al.*, which were 0.20 and −0.06, respectively. Part of the difference can be explained by our correction for other specific-heat contributions and the inclusion of spin-wave renormalization. Passenheim *et al.* measured the specific heat also for internal fields of 5.82 and 10.8 kOe. Our calculations agree with these data with an accuracy better than 5%. We have not shown these results.

A purely exchange-coupled ferromagnet with the exchange constants of Eq. (21) would exhibit a specific heat as indicated by the dashed line in Fig. 6. It is seen that the dipolar effect is less important in EuS than it is in EuO (compare Fig. 5).

The data from the present experiment deviate only a few percent from the data of Passenheim *et al.*, except below 1.1 K, where an excess specific heat develops in our experiment. We do not know the origin of this additional contribution. A least-squares fit to our data above 1.1 K gave the following exchange constants:

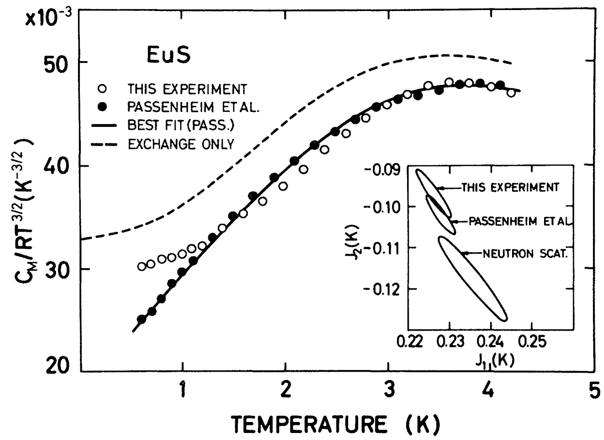

FIG. 6. Magnetic specific heat divided by $T^{3/2}$ vs temperature in EuS. The dashed curve represents the behavior of a purely exchange-coupled ferromagnet. It is seen that the dipolar effect, which causes a reduction of $C_M/RT^{3/2}$ from the dashed curve, is relatively smaller in EuS than in EuO (compare with Fig. 5 and note the suppressed zero in the present figure). The solid curve is the best fit to the data of Passenheim, McCollum, and Callaway (Ref. 3). The insert shows the covariance ellipses for J_1 and J_2 as determined from our specific-heat data (above 1 K), from the specific heat measured by Passenheim *et al.* and from the neutron scattering measurements (Ref. 6). The results of the three measurements are in reasonable agreement.

$$J_1/k = 0.226 \pm 0.004 \text{ K}, \quad J_2/k = -0.097 \pm 0.006 \text{ K}. \tag{22}$$

From the exchange constants quoted above and those determined by the neutron scattering technique[6] ($J_1/k = 0.236 \pm 0.009$ and $J_2/k = -0.118 \pm 0.011$) a set of weighted averages of J_1 and J_2 were evaluated for both EuO and EuS. These are listed as recommended values in Table IV.

Teaney and Moruzzi[22] measured the specific heats above 20 K in EuO and above 10 K in EuS, their main aim being to determine the critical behavior of the specific heat. There is no temperature overlap with the measurements dealt with in this paper, but we found it interesting to compare their results with an extrapolated calculation of the spin-wave specific heat. As already mentioned, the calculation of the spin-wave renormalization, which is included in our computation of the specific heat, agrees with direct spin-wave measurements in EuO up to 0.8 T_c.[13] It is therefore reasonable to assume that the spin-

TABLE IV. Recommended values for exchange constants.

	J_1/k (K)	J_2/k (K)
EuO	0.606 ± 0.008	0.119 ± 0.015
EuS	0.228 ± 0.004	-0.102 ± 0.005

wave specific heat can be reliably calculated in the same temperature range. We have shown such calculations in Fig. 7, plotted versus the reduced temperature T/T_c. Note that this type of curve is almost identical for the two materials, although the higher isotropy of the spin-wave energy in EuO causes this material to saturate before EuS, where there is a large spread of spin-wave energies in various directions.[6] When the spin-wave specific heat is expressed in units of R, which is the case in Fig. 7, the saturation value is unity. The dashed-dotted curve in Fig. 7 represents an average of the total magnetic specific heats for EuO and EuS above $T/T_c = 0.3$, as measured by Teaney and Moruzzi. At $T/T_c = 0.3$ the total magnetic specific heat joins smoothly to the spin-wave specific heat. We infer that the additional magnetic specific heat above $T/T_c = 0.3$ is connected with the longitudinal spin fluctuations that diverge at T_c.

B. Magnetization

The reduced magnetization was measured in EuO by Boyd[4] and in EuS by Boyd and Charap[5] using the NMR technique. Their data, reduced by $T^{3/2}$, are plotted versus T in Fig. 8. This type of plot is convenient because the reduced magnetization for a purely exchange-coupled ferromagnet expands for small T similarly to the specific heat, Eq. (18), so that the small-T behavior of $\Delta M/MT^{3/2}$ becomes linear with T. These linear dependencies were calculated for the recommended values of the exchange constants from Table IV, and are shown as dotted lines in Fig. 8. In relation to Fig. 1 we said that the magnetization below 4 K was less sensitive to the exchange than was the specific heat, and this is clearly displayed by the difference between the dotted lines and the measurements in Fig. 8. The effects of the dipolar energy are obviously not perturbations but changes by factors. Inclusion of the dipolar contribution in the spin-wave energy yielded the dashed curves in the figures. The agreement with the measurements is poor, except near 4 K in EuS. To match the observed magnetizations the spin-wave energies must be larger than those calculated from Eq. (10) with $H_{\text{int}} = 0$. An internal field of 2.4 kOe, which essentially increases the spin-wave energy at all wavevectors by about 0.028 meV ($=0.32$ K), brings the EuO calculation into perfect agreement with the measurements. However, a field of this size is an order of magnitude larger than the calculated anisotropy field in EuO,[6] and it cannot be reconciled with the specific-heat analysis.

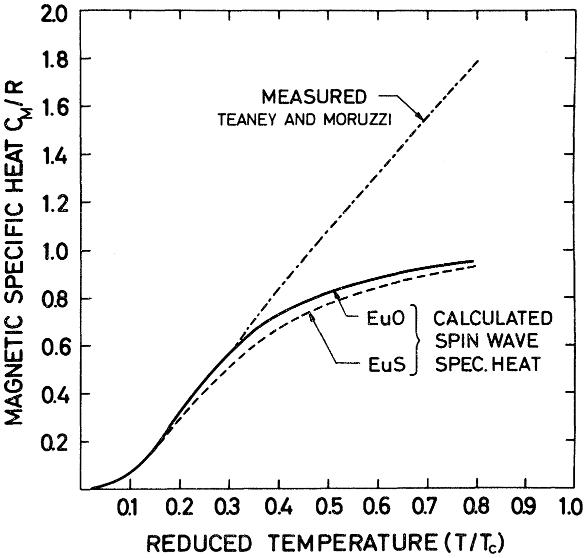

FIG. 7. Magnetic specific heats vs reduced temperature for both EuO and EuS. "Extrapolated" calculations of the spin-wave specific heat join smoothly to the total magnetic specific heat measured above $T/T_c = 0.3$ by Teaney and Moruzzi (Ref. 22). Excess specific heat above the calculated spin-wave specific heat is assigned to the longitudinal spin fluctuations.

The situation is somewhat different in EuS, because here the inclusion of an internal field (0.7 kOe in the figure) gives a temperature dependence different from that observed in the NMR experiment. To fit the observations it would be formally necessary to include a wave-vector-dependent spin-wave energy gap of about 0.01 meV at $q=0$ and with decreasing magnitude for increasing q. This is pure conjecture, of course, and we are inclined to conclude that the NMR measurements are too sensitive to effects other than the exchange energy, and that they are inferior to both specific heat and neutron scattering in respect of determination of exchange constants in EuO and EuS.

VI. CONCLUSION

Motivated by the inconsistency between the recent neutron scattering results and the specific-heat and magnetization results on the exchange

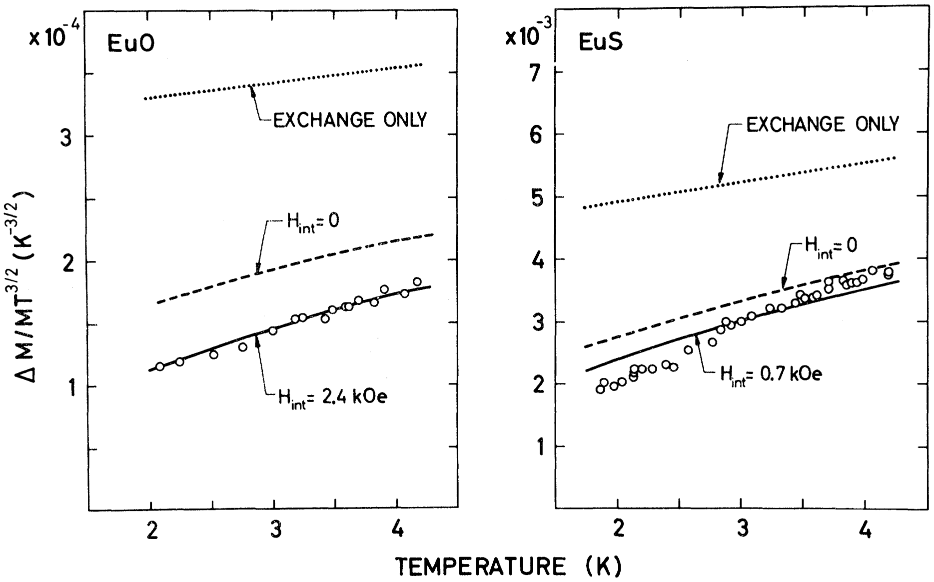

FIG. 8. Reduced magnetization divided by $T^{3/2}$ vs temperature in EuO and EuS. Points are the data of Boyd (Ref. 4) and of Boyd and Charap (Ref. 5). Dotted lines represent the behavior of a purely exchange-coupled ferromagnet. It is evident that the reduced magnetization is strongly influenced by contributions to the spin-wave energy other than the exchange. Dashed curves are calculated using the recommended values of J_1 and J_2 from Table IV, including the dipolar energy. Additional internal fields are necessary to match the observed magnetizations.

constants J_1 and J_2 in EuO, we reanalyzed the specific-heat and NMR data on EuO, and also included a reanalysis of the same type of data on EuS. It seems to us that the previous analyses had not realized the sensitivity of the bulk data to the interrelation between the two exchange constants. Thus the specific heat below 4.2 K in EuO cannot, as quoted in the previous analysis, determine J_1 and J_2 individually but only the sum $J_1 + J_2$. Our reanalysis based on all available specific-heat data on EuO, some of them previously unpublished, gave a value of $J_1 + J_2$ that is in good agreement with the neutron scattering result. From the specific-heat data we cannot check the correctness of a positive J_2 in EuO, as obtained by neutron scattering, but we have eliminated the controversial disagreement between the two techniques.

The reason that the specific heat in EuO can only determine $J_1 + J_2$ is that the measurements were not carried to sufficiently high temperatures for spin waves to be populated over the entire Brillouin zone. The situation is different in EuS, although also in this case the specific heat was measured only below 4.2 K. Because of the much lower T_c in EuS, these measurements sample the entire Brillouin zone and actually give the best determination of J_1 and J_2 in EuS (the neutron scattering technique was hampered by the large anisotropy of the spin-wave energies in EuS, because the large neutron absorption of Eu made it necessary to use a powdered sample).

We attempted an analysis of the NMR data for the reduced magnetization, but in the temperature range of the measurements (below 4.2 K) we found that the data are more sensitive to other contributions, chiefly the dipolar energy, than they are to the exchange energy. In spite of what we believe is a thorough analysis of the dipolar effects, we cannot fully account for the behavior of the NMR data without introducing additional anisotropy fields. With respect to the main aim of this paper, which was to determine the exchange constants, we excluded the NMR data as being inferior to the results of the two other techniques.

ACKNOWLEDGMENT

The authors thank Dr. T. B. Reed for the preparation of the EuO and EuS samples.

---

*Present address: General Electric Co., Hendersonville, N. C.

[1] T. Kasuya, IBM J. Res. Dev. 14, 214 (1970).

[2] A. J. Henderson, Jr., G. R. Brown, T. B. Reed, and H. Meyer, J. Appl. Phys. 41, 946 (1970).

[3] B. C. Passenheim, D. C. McCollum, Jr., and J. Callaway, Phys. Lett. 23, 634 (1966).

[4] E. L. Boyd, Phys. Rev. 145, 174 (1966).

[5] S. H. Charap and E. L. Boyd, Phys. Rev. 133, A811 (1964).

[6] L. Passell, O. W. Dietrich and J. Als-Nielsen (unpublished).

[7] F. Keffer, *Handbuch der Physik* (Springer, Berlin, 1966), Vol. XVIII/2, p. 1.

[8] N. Miyata and B. E. Argyle, Phys. Rev. 157, 448 (1967).

[9] M. C. Franzblau, G. E. Everett, and A. W. Lawson, Phys. Rev. 164, 716 (1967).

[10] T. Holstein and H. Primakoff, Phys. Rev. 58, 1098 (1940).

[11] M. H. Cohen and F. Keffer, Phys. Rev. 99, 1128 (1955).

[12] W. Marshall and S. W. Lovesey, *Theory of Thermal Neutron Scattering* (Oxford U. P., London, 1971).

[13] O. W. Dietrich, J. Als-Nielson, and L. Passell (unpublished).

[14] A. J. Henderson, D. G. Onn, H. Meyer, and J. P. Remeika, Phys. Rev. 185, 1218 (1969).

[15] Y. Shapira and T. B. Reed, J. Appl. Phys. 40, 1197 (1969).

[16] K. Y. Ahn, J. Appl. Phys. 40, 3193 (1969).

[17] D. L. Mills and A. A. Maradudin, J. Phys. Chem. Solids 30, 784 (1969).

[18] G. E. Shoemake, J. A. Rayne, and R. W. Ure, Jr., Phys. Rev. 185, 1046 (1969), and references therein.

[19] An earlier short presentation of these data has been given in Ref. 2.

[20] *Handbook of Chemistry and Physics* (Chemical Rubber, Cleveland, 1973).

[21] F. J. Dyson, Phys. Rev. 102, 1230 (1956).

[22] D. T. Teaney and V. L. Moruzzi, *Coll. Int. Centre Nat. Rech. Sci. No. 180: Les Elements Des Terres Rares, Paris-Grenoble, May 1969* (Edition du Centre Nat. Rech. Sci., Paris, 1970, Tome II, p. 131.